TALAT Lecture 1253

Creep of Aluminium and Aluminium Alloys

26 pages, 20 Figures

Advanced Level I

Prepared by S.Spigarelli
INFM/Department of Mechanics, University of Ancona,
Ancona, Italy

Objectives:

This chapter constitutes an introduction to creep and to the creep response of Aluminium and its alloys. Its major goals are:

- to provide basic information on creep and its mechanisms
- to give a description of the more extensively used mathematical relations among creep variables (time, stress and temperature)
- to illustrate the creep response of pure Aluminium and of Al-Mg alloys
- to provide a synthesis of the information available in the literature on the creep behaviour of a number of new alloys and composites in the form of a series of figures elaborated on the basis of the data reported in same sources.

Prerequisites:

Familiarity with the contents of Lectures 1201 through 1205.

Date of Issue: 1999
© EAA- European Aluminium Association

1253 Creep of Aluminium and Aluminium Alloys

Contents

1253.01 Introduction to Creep

The term **creep** indicates the **permanent, time-dependent deformation** that occurs when a material is exposed to **high temperature** under a **constant applied stress** (or load). Creep is observed in all metals, provided that the operating temperature (T) exceeds 0.3-0.5 T_M, where T_M is the absolute melting temperature. The following table lists the lower temperature limit under which creep phenomena can be neglected (pure metals). It can easily be observed that, due to its low melting temperature, Aluminium is subject to creep even at relatively low temperatures (i.e. 200-300°C).

Table I : Temperature limit above which creep is a limiting factor in design (pure metals and heat-resistant alloys).

Aluminium	**$T > 0.54\ T_M$**
Titanium	**$T > 0.30\ T_M$**
Low alloyed steel	**$T > 0.36\ T_M$**
Austenitic stainless steels	**$T > 0.49\ T_M$**
Superalloys	**$T > 0.56\ T_M$**

Creep is investigated by tension, compression or even torsion tests under constant stress or, more frequently, constant load. While constant-stress data provide a better understanding of the basic creep mechanisms, constant-load tests give more useful information from an engineering point of view (for instance, the weight of a self-loading component operating at high temperature, remains unchanged throughout its life). Temperature must obviously be maintained constant during each test, and elongation should be continuously recorded.

1253.02 The Creep Curve

Figure 1253.02.01 shows a schematic representation of a creep curve as obtained during a constant-load test. After an instantaneous deformation upon loading (ε_0), the strain increases monotonically with time up to rupture (ε_R). The overall deformation after loading can thus be written in the generic form:

$$\varepsilon = \varepsilon_0 + \varepsilon(\sigma, T, t)$$

The creep curve, i.e. the $\varepsilon(\sigma,T,t)$ component of total strain, consists of three regions:

A primary stage, or transient creep during which, in general, the strain rate ($\dot{\varepsilon} = \partial\varepsilon/\partial t$) decreases with time; in this stage, deformation becomes more and more difficult as strain increases, i.e. the material experiences strain hardening.
A secondary stage, or steady state in which the strain rate is constant ($\dot{\varepsilon} = \dot{\varepsilon}_{SS}$). The occurrence of a constant strain-rate regime is generally explained in terms of a balance between strain hardening and structure recovery (a softening process determined by the high temperature).

A tertiary stage during which strain rate increases with time, leading to the fracture of the component. The increases in creep rate during this stage result from a number of different damaging phenomena, such as cavities nucleation and growth, cracks formation, and extensive macroscopic necking. All these mechanisms produce a reduction in cross-sectional area that, under constant load, produces a continuous increase in applied stress and ultimately fracture.

Different equations have been proposed to describe the creep curve [1]; among the soundest equations, one has the form:

$$\varepsilon = \varepsilon_0 + \varepsilon_P \left[1 - \exp\left(-t / t_P\right)\right] + \dot{\varepsilon}_{SS}\, t + \varepsilon_T \left[\exp\left(t / t_T\right) - 1\right] \qquad (1)$$

where:

- ε_0 is the instantaneous elasto-plastic deformation upon loading, not associated with creep
- t is time (t=0 at loading)
- ε_P, t_P are two stress- and temperature-dependent parameters associated with the magnitude and duration of primary creep
- $\dot{\varepsilon}_{SS}\, t$ is the term for secondary creep
- ε_T, t_T are two stress- and temperature-dependent parameters associated with the magnitude and duration of tertiary creep.

Figure 1253.02.01 represents the creep curve in its more general form; yet, frequently one or two stages of the curve may be absent. For example, for some materials primary and secondary creep can be neglected, since the whole creep curve is dominated by an extensive tertiary stage. Even more frequently, secondary creep is extremely short and very difficult to identify, and in this case a "minimum creep-rate" value $(\dot{\varepsilon}_m)$ rather than a steady-state value is commonly considered.

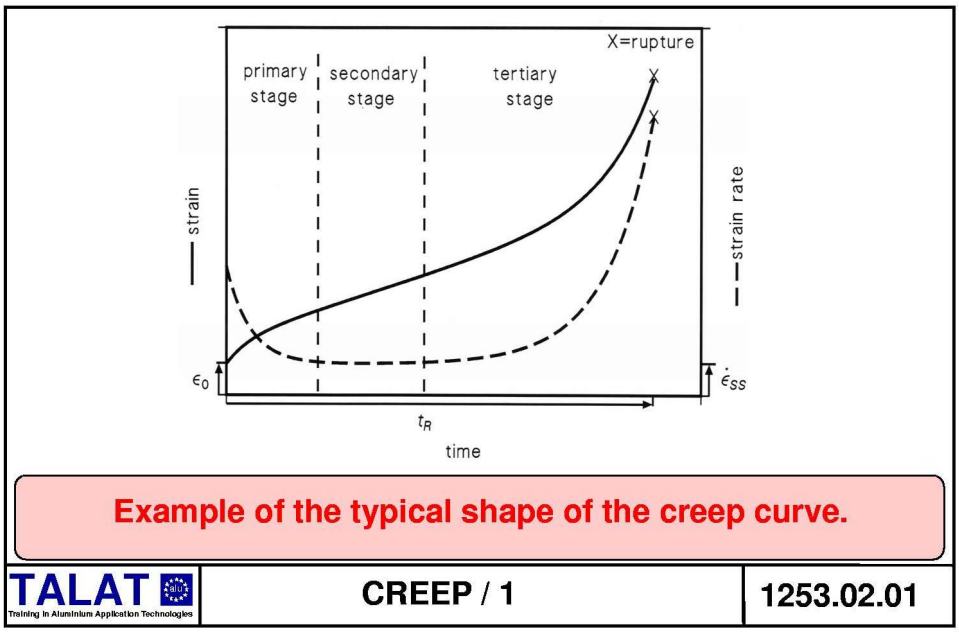

Example of the typical shape of the creep curve.

TALAT Training in Aluminium Application Technologies | CREEP / 1 | 1253.02.01

1253.03 Secondary or minimum creep rate, time to rupture

The analysis of the creep curve permits to identify the two parameters used in the engineering practice to evaluate the creep behaviour of a material. Time to rupture is perhaps the most useful from an engineering point of view, and is particularly important when creep life is the dominating concern (for example in turbine blades and rocket motor nozzles). The second parameter is steady-state or minimum creep rate. This parameter is considered when rupture, due to the low operating stress, will presumably not occur during the life of the component. In this case, in designing a component, the magnitude of the secondary creep rate can be used to evaluate the steady accumulation of strain with time in service and, with some caution, even to extrapolate the creep life of the component.

The magnitude of the minimum or steady-state creep rate is influenced by both temperature and applied stress. In particular, an increase in applied stress will correspond to a large increase in steady-state creep rate. The dependence of the steady-state creep rate on applied stress at constant temperature is commonly described by the "**power law**" equation:

$$\dot{\varepsilon}_{SS} = B\,\sigma^{n} \tag{2}$$

where B is a temperature-dependent material parameter and n, for pure metals, is 4-5. A plot of the logarithm of strain rate versus a logarithm of applied stress at different temperatures thus, results in a series of straight lines with slope n, **Figure 1253.03.01** (a). When the applied stress is particularly low, a transition to a different creep regime with n=1 is frequently observed; this transition is associated with a variation of the creep mechanism from dislocation creep (n=4-5) to purely diffusive creep (n=1).
The variation of the operating temperature also produces a significant change in the magnitude of the steady-state creep rate. This behaviour, at a given stress, is described by an equation in the Arrhenius form:

$$\dot{\varepsilon}_{SS} = C\exp\left(-Q/RT\right) \tag{3}$$

where C is a stress-dependent material parameter, R is the gas constant, and Q (activation energy for creep) for pure metals coincides with the activation energy for diffusion (Q_0). When the natural logarithm of the strain rate at different stresses is reported as a function of $1/T$, a family of straight lines with slope $-Q/R$ is obtained, **Figure 1253.03.01** (b).

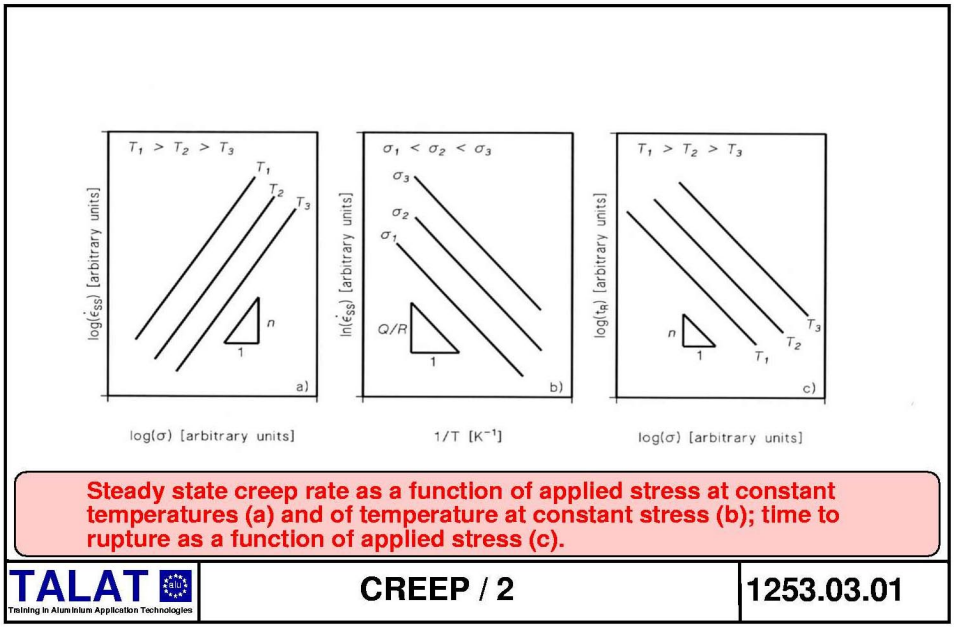

Steady state creep rate as a function of applied stress at constant temperatures (a) and of temperature at constant stress (b); time to rupture as a function of applied stress (c).

TALAT Training in Aluminium Application Technologies | CREEP / 2 | 1253.03.01

Equations 2 and 3 can be combined, giving:

$$\dot{\varepsilon}_{SS} = A\sigma^n \exp(-Q/RT) \tag{4}$$

where A is a material parameter. While in pure metals n does not depend on temperature, and Q does not depend on stress, in many engineering alloys a complex dependence of Q on applied stress, and a high or very high (7-20) value of the temperature-dependent stress exponent n are frequently observed.

1253.03.01 Diffusion and creep

Diffusion in a solid occurs because atoms can move from one atomic site to another. In particular, the atoms vibrate about their mean position with a frequency ν while, at temperature T, the average total energy for each atom is $3kT$ (where k is the Boltzmann constant). Since $3kT$ is an average value, it is easy to find atoms with higher or lower energy in any instant; thus, according to the statistical mechanical theory, the probability p that an atoms has an energy $>q$ is:

$$p = \exp\left(\frac{-q}{kT}\right)$$

Based on this expression, it can be demonstrated that, for an alloy A+B, the flow of atoms per unit time (J) between two different adjacent planes with different concentrations of the A element obeys the relationship (Fick's first law of diffusion):

$$J = -D\left(\frac{dc}{dx}\right)$$

where *dc/dx* is the concentration gradient, and *D* is the coefficient of diffusion. The *D* parameter strongly depends on temperature, and in particular:

$$D \propto \exp\left(\frac{-q}{kT}\right)$$

or

$$D = D_0 \exp\left(\frac{-Q_0}{RT}\right)$$

where $R=Nk$ and $Q_0 = Nq$ (*N* is Avogadro's number).
The diffusion data for pure metals are obtained by plating a radioactive isotope on the bulk material, by raising the temperature for a certain time and then measuring the concentration of the isotope as a function of depth in the metal.
For f.c.c metals (as Aluminium), D_0=5 x 10^{-5} m^2s^{-1}, while Q/RT_M=18.4.

The above discussion shows that atoms move in the lattice; however, atoms diffuse in several different ways. One of the most interesting mechanisms from the point of view of creep is **vacancy diffusion**; in this case, the vacancy moves from one atomic site to another, resulting in the flow of one atom in the opposite direction. This mechanism and the **diffusion of interstitial atoms** are the two ways in which **bulk diffusion** occurs. Two additional mechanisms use fast diffusion paths, i.e. the grain boundary and the dislocation core. In grain-boundary diffusion, the boundary acts as a planar channel in which the atomic distance is greater than in the lattice, providing an easy path for atom diffusion. The dislocation core itself can act in a similar way (even though the channel is rather a "pipe" of cross-section $2b^2$, where b is the Burgers vector). Since **grain-boundary diffusion** and **pipe diffusion along the dislocation core** require relatively low energy, the activation energy associated with these mechanisms is only a fraction of that for self-diffusion Q_0.

Equation 4 is widely used in theoretical studies to explain the creep behaviour of pure metals and alloys; further, it also provides very useful information on creep life (time to rupture). Indeed, provided that the creep mechanism remains unchanged in the considered stress and temperature regime:

$$\dot{\varepsilon}_{SS}\, t_R = c \tag{5}$$

where c is a constant. The combination of eqns.4 and 5 gives

$$t_R = A'\sigma^{-n} \exp(Q/RT) \tag{6}$$

where $A'=c/A$ (Fig.2c).

1253.04 Parametric Approach for Time-to-Rupture Prediction

Equation 6 can in principle be used to extrapolate time to rupture in service condition. In general, a number of different isothermal time-to-rupture vs stress curves are available (see for example Fig.3a, which shows the time-to-rupture dependence on applied stress at 426, 375 and 333 K as reported in ref. [2] for an Al-Fe-V-Si-Er alloy). Yet, frequently the limited number of isothermal curves results in the need for extrapolating creep strength at a different temperature. This problem can easily be overcome by introducing a parameter that includes two of the creep variables (usually temperature and time to rupture) as a function of applied stress.

The most widely used approach leads to the definition of the **Larson-Miller** parameter (LMP); the basic assumption is that, in eqn.3, stress dependence is included in the term Q rather than in C. Thus, by combining eqns.3 and 5, one can obtain

$$t_R = B_0 \exp\left(\frac{Q(\sigma)}{RT}\right) \tag{6b}$$

or

$$\log(t_R) = \log B_0 + \frac{Q}{RT}\log e \tag{6c}$$

After simple transformations, one can obtain

$$LMP = \frac{Q(\sigma)}{2.3R} = T\left(C_{LM} + \log t_R\right) \tag{7}$$

where C_{LM} = - log B_0 is a constant which, for many materials including steels, is set =20 **Figure 1253.04.01** (b) shows the same data as **Figure 1253.04.01** (a), reported in the form of the Larson-Miller parameter. All the experimental points collapse, with tolerable dispersion, on the same **Master Curve**, which can be used to evaluate the creep strength (stress that a given temperature produces a given time to rupture) of the alloy.
Other approaches result in different parameters: for example, the Dorn-Orr-Sherby parameter (here identified as DOSP) is defined as:

$$DOSP = \log t_R - \frac{Q}{2.3R} \tag{8}$$

This parameter has the best physical basis, but the LMP is the most widely used in engineering practice.

For the correct extrapolation of the creep strength of an alloy, a sufficiently broad matrix of test results must be available (in particular, long-term creep data should also be included in the calculation of the master curve). Thus, the curves in
Figure 1253.04.01 must be considered only as explanatory examples, and are of very limited engineering use.

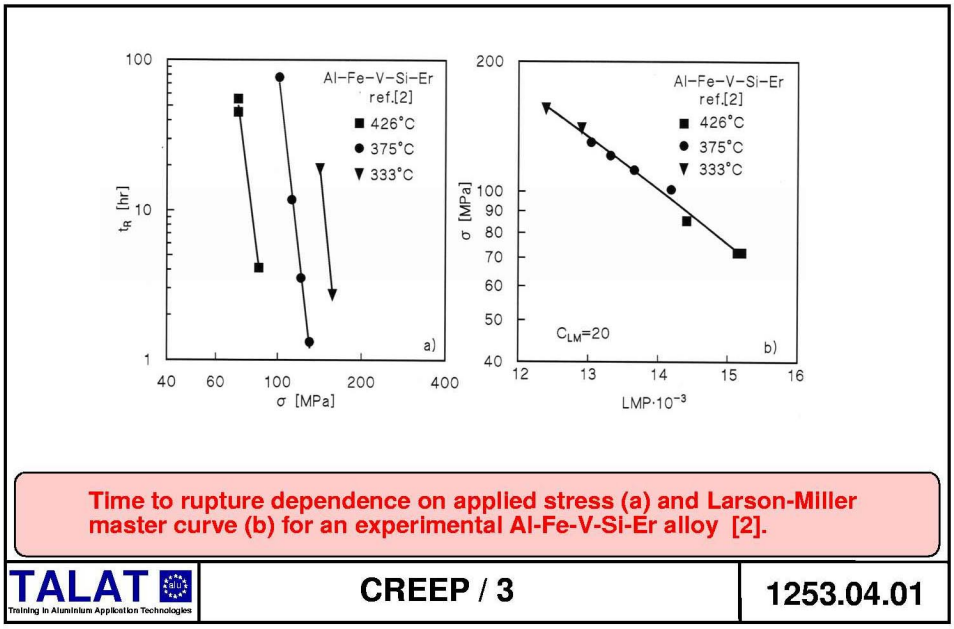

Time to rupture dependence on applied stress (a) and Larson-Miller master curve (b) for an experimental Al-Fe-V-Si-Er alloy [2].

1253.05 Creep mechanisms: pure metals (class M) and solid solutions (class A)

Equation 4 provides a good description of the stress- and temperature-dependence of steady-state (or minimum) creep rate. Yet, a slightly more complicated and general form of the same equation [3]:

$$\dot{\varepsilon}_{SS} = A_0 \frac{D_0 G b}{kT}\left(\frac{b}{d}\right)^p \left(\frac{\sigma}{G}\right)^n \exp\left(\frac{-Q_0}{RT}\right) \qquad (9)$$

is frequently used to describe the creep response of Aluminium and its alloys. In eqn.9 A_0 is a dimensionless material parameter, b is the Burgers vector, d is the grain size, G is the shear modulus, k is the Boltzmann constant, D_0 is the frequency factor (i.e., being D the appropriate diffusion coefficient, $D=D_0\exp(-Q_0/RT)$), n and p are constants.

According to refs. [3-4], the creep behaviour of a **pure metal** (and of a number of alloys indicated as **class-M materials**) can be divided into three stress regimes, **Figure 1253.05.01** :

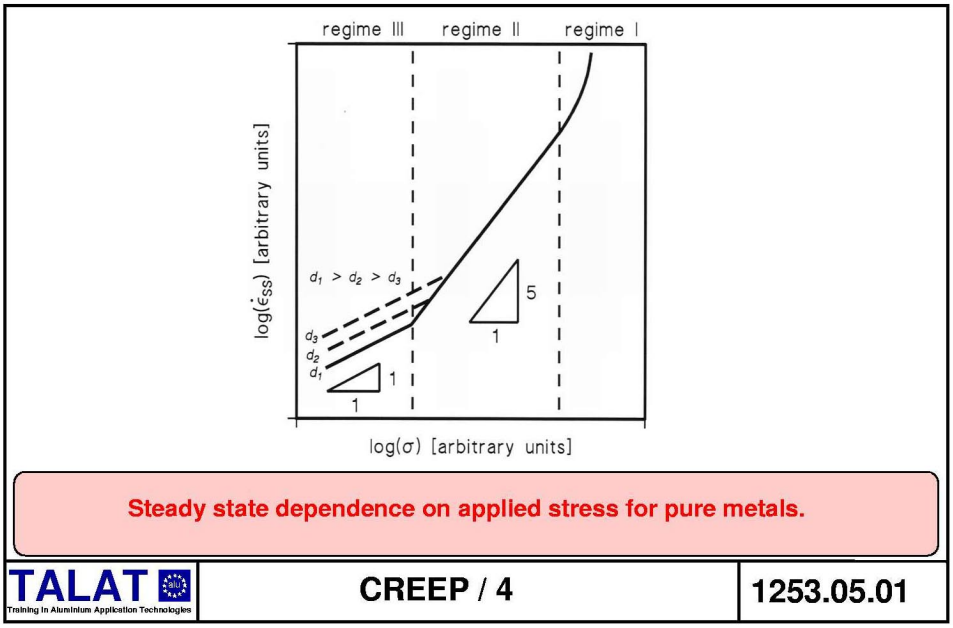

Steady state dependence on applied stress for pure metals.

TALAT Training in Aluminium Application Technologies | CREEP / 4 | 1253.05.01

I a high-stress regime, where the conventional power law (eqn.4or 9) should be replaced with an exponential dependence of the strain rate on applied stress. This regime is not particularly important in creep due the very high strain rate involved, but is rather a primary concern in hot-forming operations.

II an intermediate-stress regime, characterised by a stress exponent n=4-5, p=0 and a value of Q=Q_0 (Q_0 is the activation energy for lattice self-diffusion). In this regime creep is controlled by recovery mechanisms, such as **climb** and **annihilation of dislocations** (**Figure 1253.05.02).** The edge dislocations can climb due to the extensive diffusional flow of vacancies; then the high temperature enhances the mobility of dislocation, and diffusion controls the creep strain rate (thus explaining the coincidence between Q and Q_0). In fact, the deformation results from a sequence of glide and thermally-assisted climb; the slowest mechanism is rate controlling, and as long as glide is very easy (as in pure metals), creep is controlled by climb.

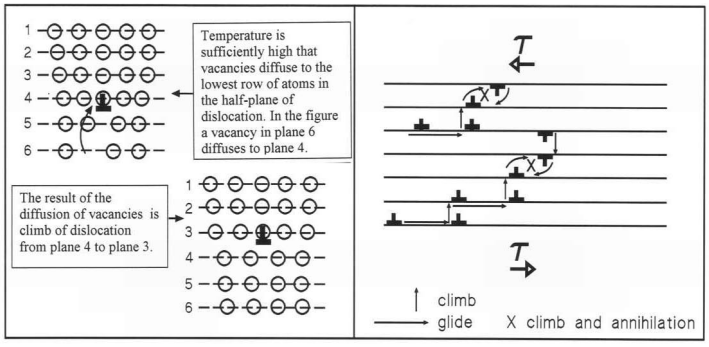

Mechanisms of climb controlled creep: a dislocation climbs on a parallel plane due to diffusion of vacancies; the climb-glide sequence leads to creep.

TALAT Training in Aluminium Application Technologies | CREEP / 5 | 1253.05.02

III a low stress regime, in which n=1. Two different, purely diffusive (no dislocation) mechanisms have been identified in this region (**Figure 1253.05.03).** In Nabarro-Herring creep, the diffusional flow of vacancies through the grain results in the elongation of the grain itself in the direction of applied stress; in this case n=1, p=2 and $Q=Q_0$. In Coble creep the elongation of the grain structure is the result of diffusion of vacancies along the grain boundary, giving n=1, p=3 and $Q=0.6Q_0$. In both cases, the flow of vacancies occurs from the grain boundaries perpendicular to the boundaries parallel to the stress axis [3,5]. In many metals an additional mechanism, known as Harper-Dorn creep, results in a value of n=1 (but with p=0); this last mechanism involves a form of dislocation activity and must be not confused with purely diffusive creep.

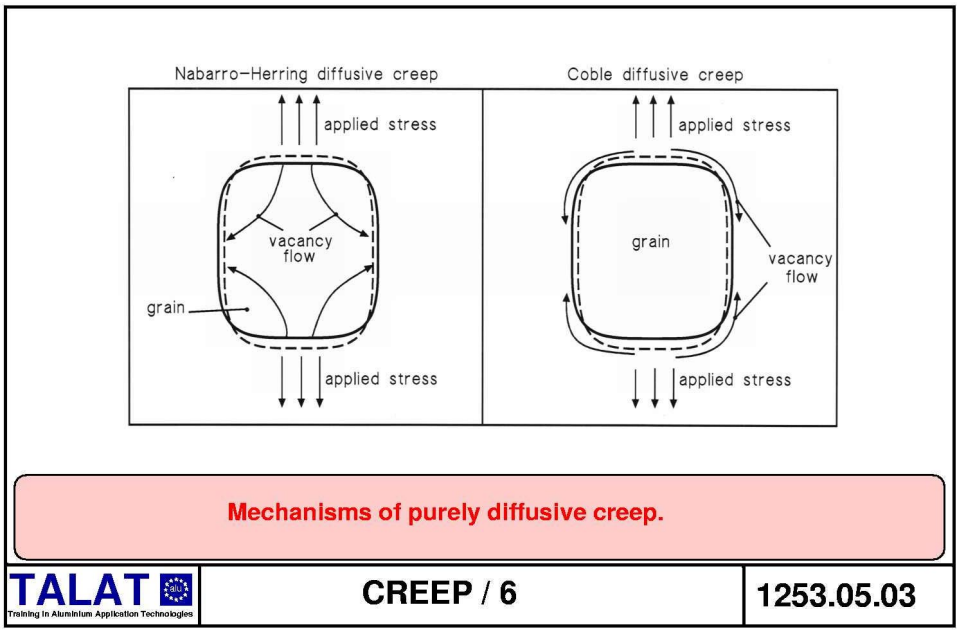

In all the above regimes, operates a further mechanism (grain-boundary sliding). In coarse-grain metals, grain-boundary sliding produces a relatively negligible fraction of the total strain, but could be responsible for intergranular creep fracture. Only in very fine-grained materials (submicron grain size) does grain-boundary sliding become the dominating mechanisms and result in very large deformation (superplasticity). In this case, n=2.

In **solid-solution alloys** (**class-A materials**) the creep-rate dependence on applied stress is somewhat more complicated. In particular, the following regimes can be identified (**Figure 1253.05.04**):

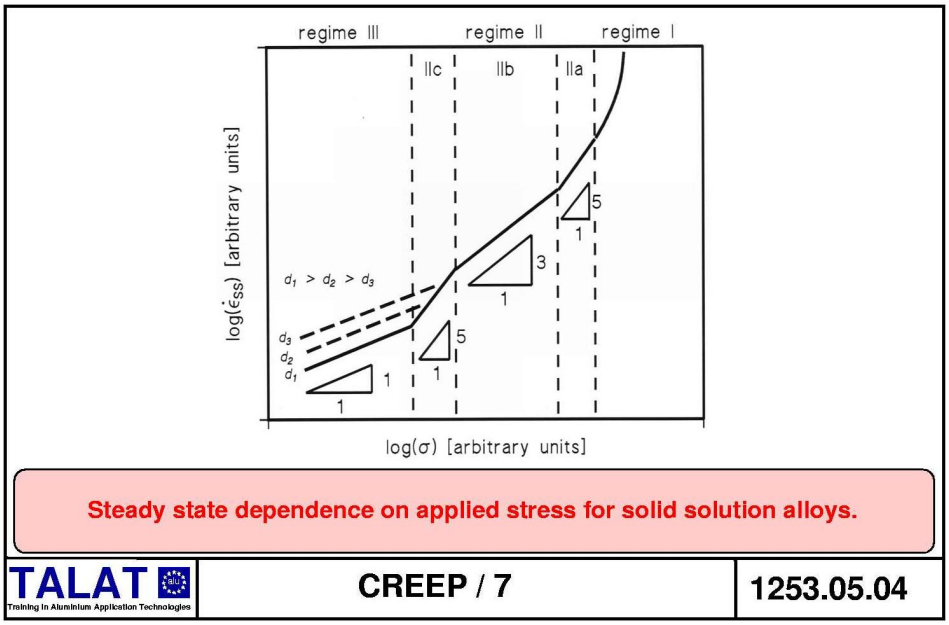

I the very high-stress regime characterised by power law breakdown

IIa a first region of the intermediate-stress regime, where creep is controlled by climb (n=4-5, Q=Q_0)

IIb a second region of the intermediate-stress regime, where creep is controlled by glide of dislocation in a "cloud" of solute atoms ("viscous drag"); in this regime climb is faster than viscous glide, and n=3, p=0 and Q=Q_0

IIc a third region of climb-controlled creep (n=4-5, Q=Q_0)

III the low-stress, purely diffusive or Harper-Dorn creep regime.

As in pure metals, glide of dislocation and climb occur in sequence. In region IIc, climb is the slowest mechanism and is rate controlling. When applied stress increases, the climb of dislocations becomes faster and faster, and viscous drag is the slowest mechanism (region IIb). In region IIa, the applied stress is sufficiently high for dislocations to break away from their solute-atom atmospheres and glide easily.

The above discussion outlines some of the most striking differences between the creep response of pure metals and class-M alloys, and solid-solution alloys of class A. Yet, even more pronounced are the differences in microstructural evolution during primary creep. In class-M materials, a "normal primary creep" (similar to that illustrated in **Figure 1253.02.01**) is associated with the rearranging of dislocations to form a well-defined substructure (subgrains). In class-A materials, dislocation distribution during primary creep remains homogeneous, and very often there is a short initial stage during which the strain rate increases instead of decreasing [3,5].

1253.06 Methods to Improve the Creep Strength of a Metallic Material

According the above concepts, in selecting a metal able to withstand dislocation creep, the following criteria should be followed:

- choosing a material with a high melting point

- reducing dislocation mobility by adding obstacles

In selecting a material able to resist diffusional flow, partially different criteria should be preferred:

a) choosing a material with a high melting point
b) producing a large grain size, reducing the volume fraction of grain boundaries. In this case, a long diffusion path is required for grain-boundary diffusion. Further, a large grain size reduces the contribution of grain-boundary sliding (submicron grain size should be avoided in this sense).
c) inducing by proper alloying and heat treatment the precipitation of particles on grain boundaries, thus introducing a further obstacle to grain-boundary sliding. A continuous chain of precipitates should nevertheless be avoided, since it constitutes an easy path for cracks.

According to this scheme, the most widely used methods to improve tensile strength at room temperature very often do not result in increased creep strength. For example:

1. the **reduction of the grain size** strengthens the material at low temperature, but could be dangerous in creep.
2. **cold working** increases tensile strength at low temperature; yet, exposure to sufficiently high temperature produces recovery or even recrystallisation, with resulting softening. Thus, cold working is effective in enhancing creep strength only at moderately low temperatures.
3. the **precipitation** of secondary-phase particles enhances both tensile strength and creep response. Fine particles can obstruct dislocation mobility, thus reducing creep. Yet, prolonged exposure to high temperature causes the coarsening of the precipitates, with progressive loss of the hardening effect

The addition of a solid-solution element usually slightly improves the creep response of a metal, but the most efficient method to increase the low creep strength typical of pure metals is to introduce a **dispersion of fine and stable particles**. These particles could be the result of a precipitation process (as in Nickel-base superalloys) or can be introduced via powder metallurgy. The stable dispersion of oxides, carbides or even reinforcements (as in composites) greatly enhances creep strength. For these materials, when a sufficiently broad range of experimental data is obtained, the steady-state creep-rate dependence on applied stress appears as in **Figure 1253.06.01**. In an intermediate-stress regime, very high values of the stress exponent are observed and when Q is calculated in this region, a value largely higher than Q_0 is obtained. The extrapolation of the curve up to very low values of strain rate permits very often to identify a "threshold stress" under which creep should not occur [5].
Several approaches have been proposed to describe the strengthening effect of stable precipitates on creep; the most widely used model is based on the equation:

$$\dot{\varepsilon}_{SS} = A'_0 \frac{D_0 G b}{kT} \left(\frac{\sigma - \sigma_{Th}}{G} \right)^n \exp\left(\frac{-Q_0}{RT} \right) \qquad (10)$$

which is formally similar to eqn.9 where the applied stress is replaced with an effective stress $\sigma - \sigma_{Th}$, where σ_{Th} is a temperature-dependent threshold stress. The

stress exponent n should be the same for the base alloy (i.e. the "matrix") and the reinforced material in the same range of effective stress (for example, n=5 for pure metals and class-M alloys reinforced with stable particles). The magnitude of the threshold stress is commonly associated with one of the mechanisms by which dislocation by-passes particles (cutting, Orowan by-pass, climb).

When the applied stress is decreased below the value of the threshold stress, a change in creep mechanisms normally results; for example, a threshold stress could divide two different regimes, in which dislocation can by pass particles or dispersoids via climb (low stresses) or Orowan mechanism (high stresses). Alternatively, as shown in **Figure 1253.06.01** , a threshold stress can divide a high-stress regime in which dislocation creep (and particle-dislocation interaction) dominates, from a low-stress regime of Coble/Harper-Dorn/Nabarro-Herrring creep.

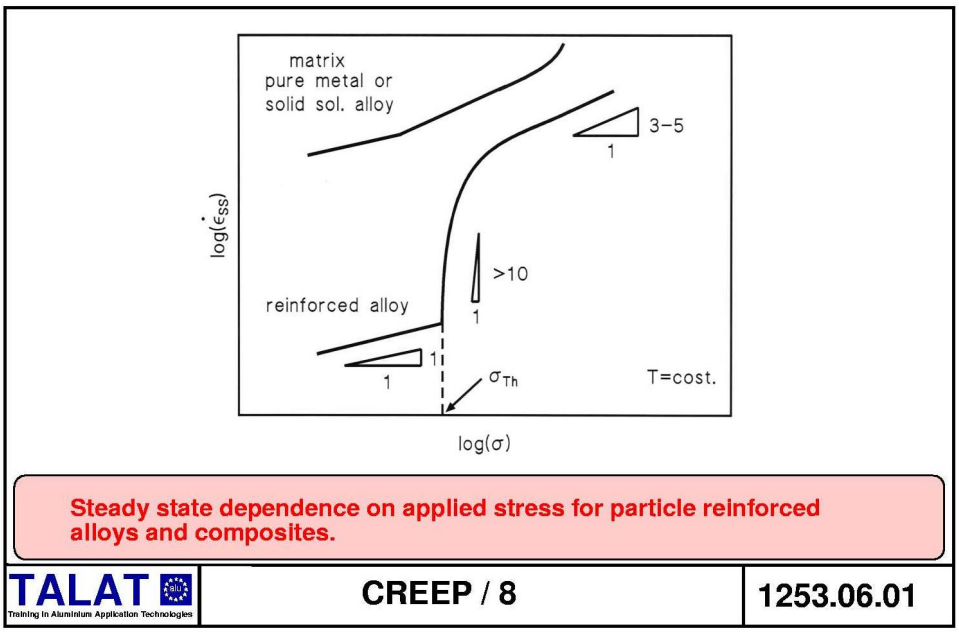

1253.07 Creep Rupture

Creep rupture occurs as a result of different and sometimes concurring mechanisms. The fractured sample, for instance, can show extensive necking (i.e. the fracture is of the conventional ductile type typical of non-brittle metals at room temperature). By proper variation of stress and/or temperature, the same material could equally experience creep rupture with negligible necking, showing all the features typical of **intergranular fracture**. This latter case is particularly interesting because it is typical of creep. As previously observed, **grain-boundary sliding** is one of the characteristic features of creep: **Figure 1253.07.01** shows two cases in which, under a certain tensile stress, grains slide one over the other; in both examples, grain-boundary sliding produces a cavity, located on the grain boundary approximately **perpendicular to the stress axis**. The two cavities have a different shape: the sharp crack formed in a triple junction of grain boundaries is defined as **type w** (wedge crack), while the round cavity produced on a step in grain boundary is defined as **type r** (round cavity).
The coarsening and growth of such cavities and/or cracks results in a reduction of the cross-sectional area, and leads to an intergranular fracture with low or no necking.

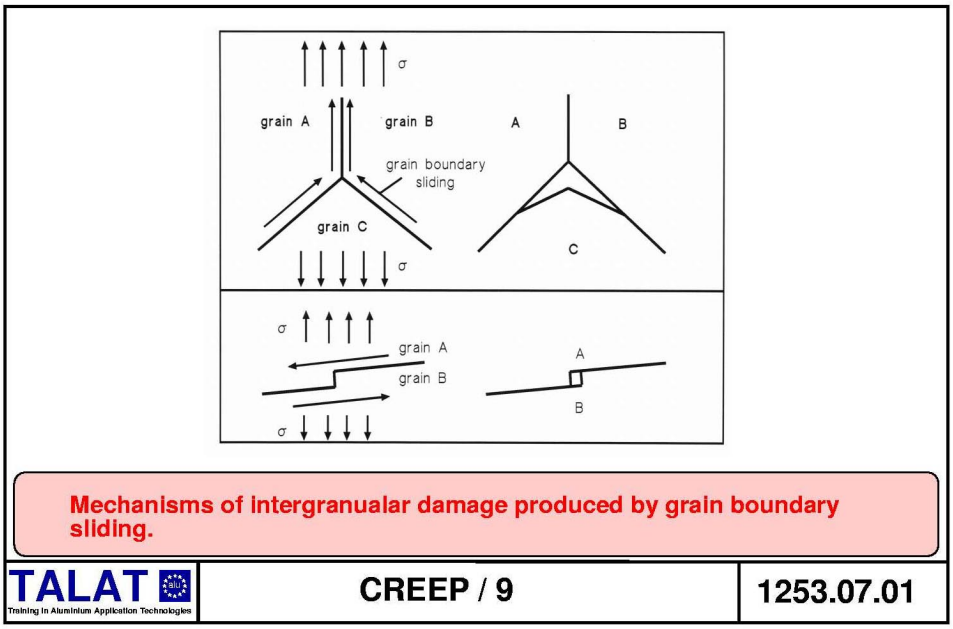

1253.08 The Creep Response of Pure Aluminium

Pure Aluminium has been extensively studied to evaluate the basic creep mechanisms in f.c.c. metals. The engineering value of pure metals is rather negligible, and rupture strength is consequently of no concern; thus, the majority of available data are in the form of secondary-creep rate vs stress. A collection of data obtained from different sources has been elaborated in ref.[6]; in this case eqn.4 was reformulated giving:

$$\dot{\varepsilon}_{SS} \exp\left(\frac{Q}{RT}\right) = A'\left(\frac{\sigma}{G}\right)^n \qquad (11)$$

Taking $Q=Q_0$=142 kJ/mol (activation energy for self-diffusion in Aluminium), all the data from different authors collapsed on the same curve (**Figure 1253.08.01**). The stress exponent in the high-stress regime is close to 5, a clear indication of climb-controlled creep.
Evidences reported in ref.[3] clearly suggests that in the low-temperature regime the stress exponent n=1 identifies Harper-Dorn creep rather than purely diffusive mechanisms.

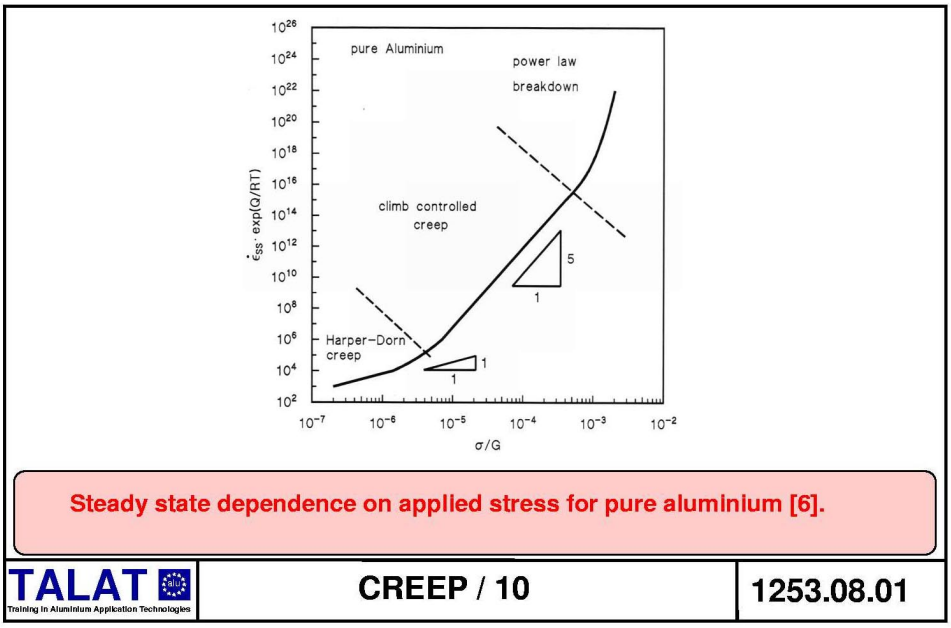

Steady state dependence on applied stress for pure aluminium [6].

TALAT Training in Aluminium Application Technologies | CREEP / 10 | 1253.08.01

1253.09 The Creep Response of Al-Mg Solid-solution Alloys

As in pure Al, the study of the creep behaviour of Al-Mg solid-solution alloys has focused on the basic creep mechanisms. A considerable body of data obtained with different alloys (with variable Mg content) is available in the form of steady-state strain rate vs stress. As expected, in a relatively large interval of applied stress, creep is controlled by viscous glide of dislocation (**glide of dislocation in an atmosphere of Mg atoms**).

The coexistence of regions IIa, IIb and IIc in the intermediate-stress regime is clearly illustrated, for an Al-2.2 at.%Mg, in **Figure 1253.09.01** (a) [7]. The increase in Mg content, on the other hand, reduces strain rate increasing creep strength (Figure 1253.09.01 (b), ref.[8]); further, the increase in the amount of Mg atoms in solid solution shifts the transition between regions IIa-IIb and IIb-IIc (i.e. the viscous-glide region extends when the solute concentration is increased). A low amount of Mg in solid solution, is thus a prerequisite for clearly recognising climb-controlled creep, since at 5.5 at.% region IIc is extremely short, and region IIa disappears (**Figure 1253.09.02**, material tested in shear, data from ref.[9]). As expected, the microstructure of the alloy is substantially different in the regions with n=4.4 and n=3; in the climb-controlled creep regime, there is clear evidence of subgrains formation, while in the viscous-glide region the dislocation distribution remains substantially homogeneous.

Under very low applied stress, the low stress exponent indicates Harper-Dorn creep.

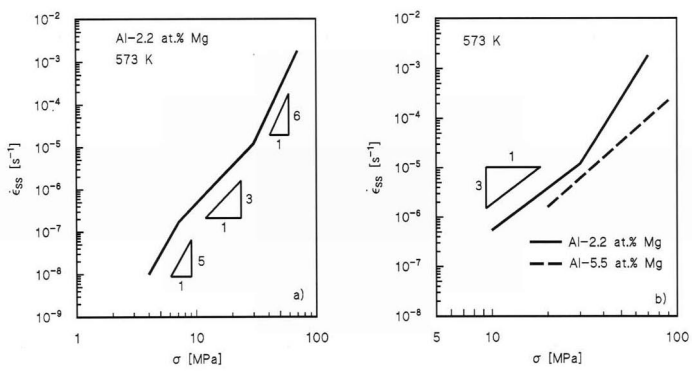

Steady state dependence on applied stress for Al-Mg solid solution alloys [7-8].

TALAT Training in Aluminium Application Technologies | CREEP / 11 | 1253.09.01

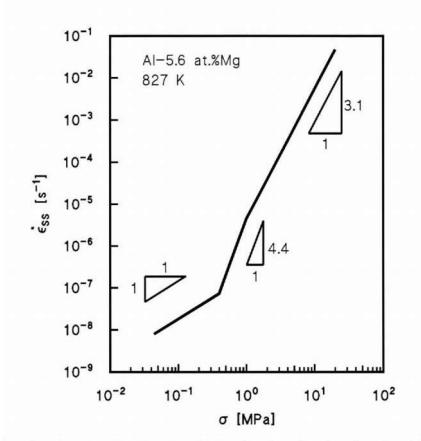

Steady state dependence on applied stress for Al-Mg solid solution alloys [9].

TALAT Training in Aluminium Application Technologies | CREEP / 12 | 1253.09.02

1253.10 The Creep Response of High Strength Aluminium Alloys

In Aluminium alloys an increase in tensile strength can be achieved by **cold working** or **precipitation hardening**. The Aluminium alloys that do not respond to heat treatment can be strengthened by introducing a dislocation substructure by a suitable cold-forming procedure. In this case, the strengthening effect is progressively lost when temperature is increased; indeed, as previously observed, cold working cannot be considered a fully satisfactory method to increase creep strength since prolonged exposure to a sufficiently high temperature produces recovery or even recrystallisation.

Heat-treated Aluminium alloys undergo an age-hardening heat treatment that determines a fine dispersion of precipitates which in turn effectively reduce the mobility of dislocations. As long as the size of the precipitates is stable, this procedure

also increases the creep strength of the alloy; precipitation-hardened alloys, are in fact aged at the temperature that allows the peak properties to be obtained in relatively short time. If the material is exposed to a temperature close to the ageing one, precipitates will rapidly grow and coarsen, and the alloy eventually softens, a typical feature of overageing. For this reason, the maximum allowable temperature for this group of alloys should be substantially lower than the final ageing temperature. An example of this behaviour is clearly illustrated in
Figure 1253.10.01, which reports the Larson Miller parameter as obtained for Aluminium (1050 alloy) and a 2XXX heat-treated alloy. The latter, in particular, was solution-treated, cold-worked and then aged to produce a fine dispersion of precipitates nucleated on dislocations. Such a treatment significantly raises tensile strength, but also strongly increases creep strength at low temperature/short time of exposure. Yet, when the alloy is exposed to temperatures exceeding 300°C, creep strength progressively approaches the one typical of Aluminium. **Figure 1253.10.01** clearly illustrates that when low-temperature short-term creep data (low values of the LMP) are used to extrapolate the creep behaviour at higher temperatures (broken line), a substantial overestimation of creep strength is obtained. This behaviour reflects the instability of the precipitates, which at temperatures higher than 300°C coarsen and lose their strengthening effect.

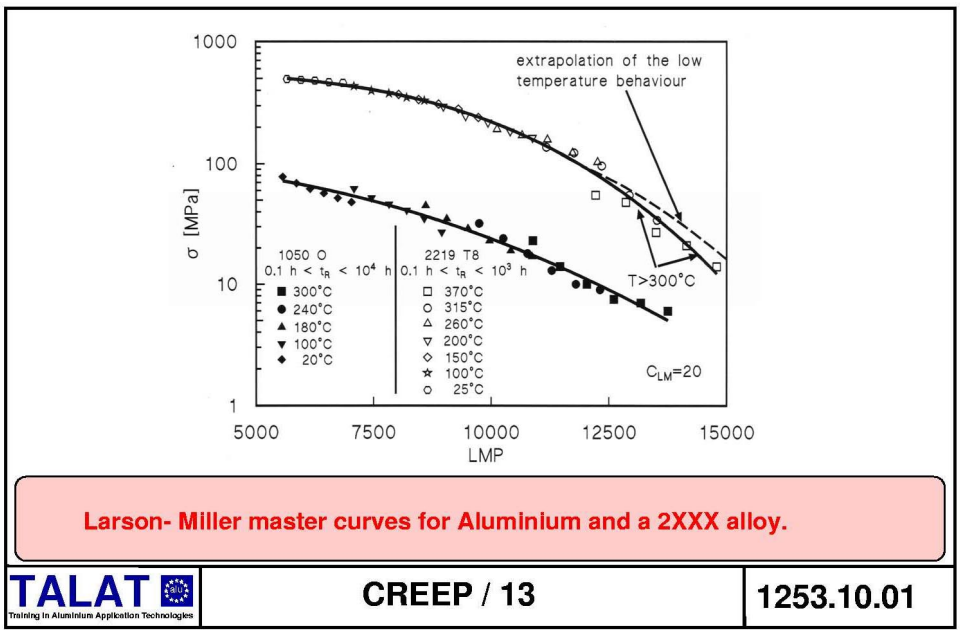

To raise the low maximum allowable temperature for 2xxx alloys, other alloying elements have been introduced, such as Ni and Fe, to form intermetallic compounds ($FeNiAl_9$) that stabilise and strengthen the structure. The 2618 (RR58) alloy was thus introduced to resist prolonged exposure (50 000hr) to moderately high temperatures; however, even in this case the maximum allowable temperature did not exceed 120°C. An additional problem typical of age-hardened alloys is their susceptibility to grain-boundary damage; in particular, the region adjacent to the grain boundary is often softer than the grain interior due to the presence of a precipitate-free zone. Moreover, the presence of hard particles on grain boundaries (a common feature in these alloys) promotes the formation of "r" cavities.

In recent years, a major effort has been devoted to investigating the creep response of a number of Aluminium alloys produced by powder-metallurgy techniques. These

alloys include several heat-resistant materials reinforced with stable particulates, as well as alloys of "conventional" composition but produced by powder metallurgy. Alloys such as 2124 [10], 2024 and 6061 [11] can successfully be used as matrix for composites; since the complete characterisation of the reinforced material should include a detailed knowledge of the creep response of the unreinforced material, these alloys have been extensively studied. A common feature of the creep behaviour of these materials is the steady-state creep-rate dependence on applied stress; **Figure 1253.10.02** shows a comparison between the steady-state creep rate for a 2024 produced by powder metallurgy and two Al-Mg solid-solution alloys. The experimental variation of steady-state creep rate with stress is substantially similar to the one observed in particle-reinforced materials (see **Figure 1253.06.01**). In this case, the presence of a threshold stress should be attributed to the effect of extremely fine particles precipitated during creep and/or to very fine Al_2O_3 dispersoid produced during powder processing. In fact, the high reactivity of Aluminium with Oxygen results in the formation of a stable oxide layer on powder particles. Subsequent extrusion breaks up this oxide layer and disperses fine fragments in the bulk of the alloy. Yet, the threshold stress depends strongly on temperature, an effect that is explained with difficulty by current theories.

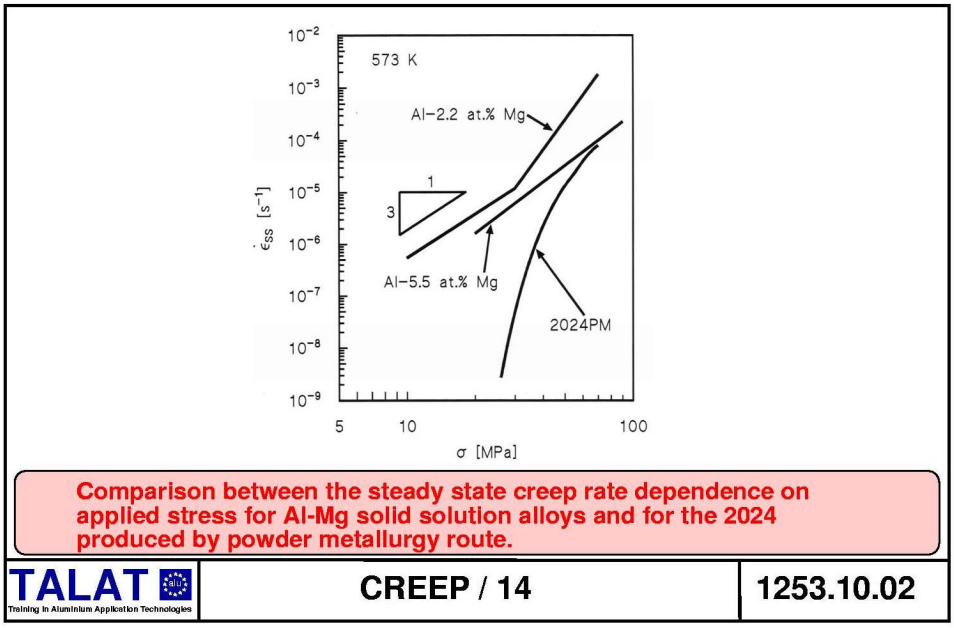

Comparison between the steady state creep rate dependence on applied stress for Al-Mg solid solution alloys and for the 2024 produced by powder metallurgy route.

TALAT Training in Aluminium Application Technologies | CREEP / 14 | 1253.10.02

1253.11 Creep-resistant Al-base Materials: High-strength Powder Metallurgy- Dispersion-strengthened Aluminium Alloys

In recent years, the introduction of two new technologies, **Rapid Solidification** and **Mechanical Alloying**, have resulted in the production of several experimental Aluminium alloys designed for high-temperature application. The major goal in developing these new materials was coupling the low weight typical of Al alloys with greater creep strength due to a dispersion of stable particulates. Current high-strength Aluminium alloys produced by ingot metallurgy, such as 2618, 2219 or other 2XXX alloys, rely on a dispersion of precipitates (Al_2CuMg or Al_2Cu) to achieve high tensile properties; nonetheless, these precipitates are unstable, and if exposed to high temperatures they coarsen, determining the softening of the alloy. By contrast, the new

powder-metallurgy high-temperature alloys contain a fine dispersion of stable particulates (for example Al_2O_3) that do not coarsen during creep.
A large number of new experimental alloys of different families have been produced and tested: for example Alcoa [12] studied the Al-Cr, Al-Mn, Al-Fe, Al-Co, Al-Ni, Al-Ce, Al-Cr-Mn, Al-Cr-Fe, Al-Cr-Co, Al-Cr-Ni, Al-Cr-Ce, Al.Mn-Fe, Al-Mn-Co, Al-Mn-Ni, Al-Mn-Ce, Al-Fe-Co, Al-Fe-Ni, Al-Fe-Ce, Al-Co-Ni, Al-Co-Ce and Al-Ni-Ce systems. The result of this preliminary study led to the selection of some alloys of the Al-Fe-X systems (where X could be Co, Ni, Ce or a mixture of rare earths). The analysis of their high-temperature properties (including creep strength) has yielded encouraging results, showing significant improvement with respect to conventional 2XXX alloys, even though ductility, toughness and fatigue-crack growth remain major concerns. The Al-Fe-Ce alloys, in particular, have been selected for further development to meet properties requirements in compressor impellers for APUs (Auxiliary Power Unit) [13].

Figure 1253.04.01 shows one of the examples of the data available for the Al-Fe family of high-strength alloys produced by powder metallurgy [2].
Figure 1253.11.01 shows the steady-state creep-rate dependence on applied stress for the same Al-Fe-V-Si-Er alloy (Al-8.5%Fe-1.3%V-1.7%Si-0.75%Er, wt.%); this alloy is a further development of the older Al-Fe-X system, with further improved stability of the $Al_{13}(Fe,V)_3Si$ precipitates. The addition of Er aimed at increasing ductility and tensile strength. As noted for time-to-rupture data, the test matrix at the two extreme temperatures is very limited; yet, the data obtained at 375°C closely follow the trend illustrated in **Figure 1253.06.01** (the slope of the curve obtained at this temperature increases from 14 to 24 when stress decreases). The activation energy for creep, Q, exceeded 340 kJ/mol, as expected in this particle-strengthened material.

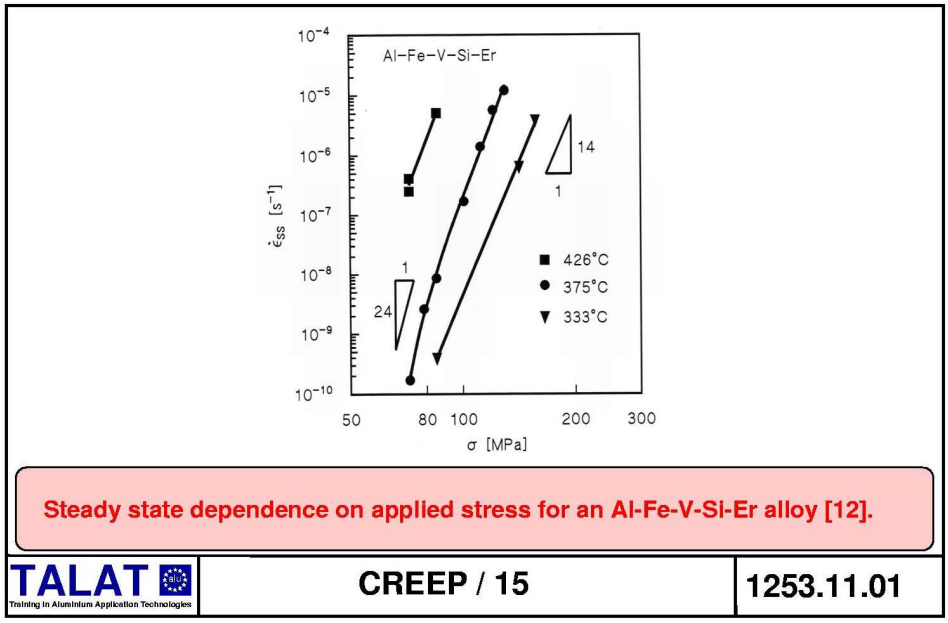

Similar investigations were carried out on other Al-Fe-V-Si alloys (Al-11.7%Fe-1.15%V-2.4%Si) [14]; again the steady-state creep-rate dependence on applied stress can be described by a power law with a stress exponent increasing from 13 to 32 as temperature decreases from 479 to 237°C (**Figure 1253.11.02**). The activation energy for creep was found to be close to 360 kJ/mol.

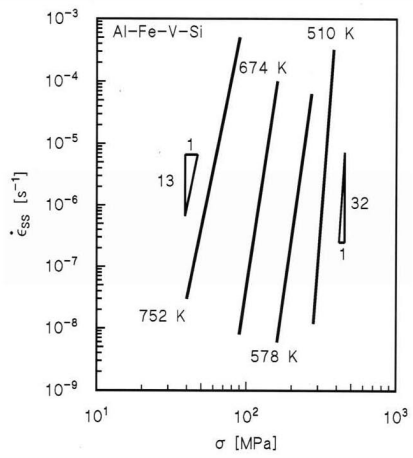

Steady state dependence on applied stress for an Al-Fe-V-Si alloy [14].

TALAT Training in Aluminium Application Technologies | CREEP / 16 | 1253.11.02

Another group of intensely studied dispersion-strengthened aluminium alloys is characterised by the presence of Aluminium carbides as the reinforcing phase. The production route for these alloys is based on reaction milling, while their composition may vary from a relatively simple Al-0.031%C-0.98%O alloy [15] to a more complex Al-4%Cu-1.5%Mg-1.2%C-0.75%O [16]. The role of Carbon is to combine with Al to form Al_4C_3, a phase that is thought to increase the creep strength more effectively than MgO or Al_2O_3. **Figure 1253.11.03** illustrates the typical behaviour of this family of alloys at two different testing temperatures (compression tests) [15]; again, the experimental behaviour is consistent with the qualitative description of **Figure 1253.06.01**, since there is clearly a region characterised by very high stress exponents and activation energy for creep (n=15-200, Q>700 kJ/mol), and, in certain experimental conditions, a low stress regime of creep with n=1. It should be mentioned that the response of these materials has been described by different models (based, for example, on the concept of thermally activated dislocation detachment from dispersoids [15]), rather than by the conventional eqn.10, since the existence (and nature) of the threshold stress is still controversial. An additional feature on these particle-reinforced alloys is the substantial difference between tensile and compression data [17], an effect that can be attributed to the microstructural anisotropy of the material.

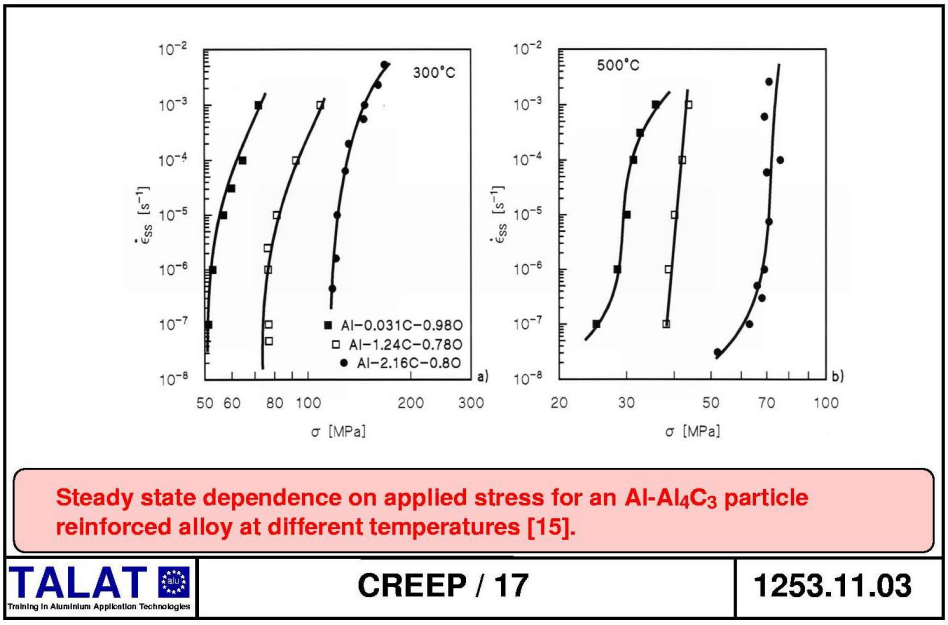

Steady state dependence on applied stress for an Al-Al_4C_3 particle reinforced alloy at different temperatures [15].

TALAT | CREEP / 17 | 1253.11.03

As a final example of reinforced Al alloys, the family of materials reinforced by Al_2O_3 particles should be mentioned (indeed, when the volume fraction of reinforcement is sufficiently high, i.e. 10-20%, these particle-reinforced alloys could in principle be regarded as composites). **Figure 1253.11.04** (a) (reporting the steady-state creep rate as a function of applied stress for an Al-Al_2O_3 alloy) illustrates a further example of coexistence of two regimes; a high-stress regime with the features of a particle-strengthened material (compare with **Figure 1253.06.01**), including a very high value of the activation energy (370 kJ/mol), and a low-stress regime characterised by a lower value of activation energy for creep (85 kJ/mol) [18]. A similar behaviour was observed in an Al-15%Al_2O_3 (% in volume) produced by mechanical alloying: again, the very high value of the stress exponent (n=25) indicates effective strengthening due to the particulate. Only in the low stress regime does a low value of the stress exponent and of the activation energy for creep (n=2, Q=46 kJ/mol) suggest that grain-boundary sliding is rate controlling (**Figure 1253.11.04** (b) [19].

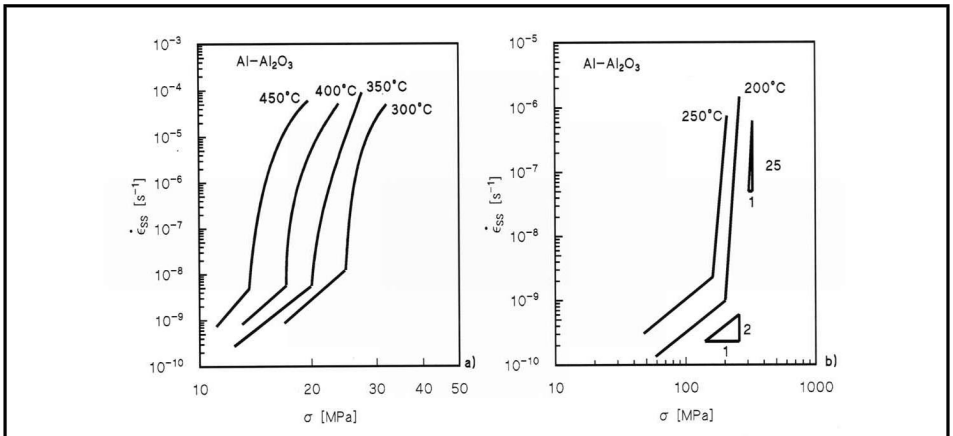

Steady state dependence on applied stress for an Al-Al_2O_3 particle reinforced alloy at different temperatures: a) ref. [18]; b) ref. [19].

TALAT | CREEP / 18 | 1253.11.04

1253.12 Creep-resistant Al-base Materials: Composites

The last group of creep-resistant Al-base materials is constituted by composites. This family of materials includes a number of different matrix- (pure Al, Al-Mg, 2XXX or 6XXX alloys) -reinforced by particles (usually SiC or Al_2O_3) or short fibres (SiC). Several approaches have been employed, including finite-element modelling of the interaction between matrix and reinforcements, and the conventional study of the steady-state creep rate as a function of stress and temperature. In general none of the approaches has given fully satisfactory results; yet, an extensive study of contemporary results has shown that the majority of creep data can successfully be described by means of the phenomenological eqn.10 (with n=3 or 5, and Q=Q_0=142 kJ/mol) [20]. Rather, the strong dependence of the calculated threshold stress has remained unexplained, in keeping with its nature; in fact, the size of the reinforcements (as in many particle-reinforced materials) is usually too large for a direct interaction with dislocations to be invoked. Nevertheless, the same approach has been used also in more recent studies [21-22].

Some examples of the behaviour of Aluminium-matrix composites are illustrated in Fig.19 and 20. **Figure 1253.12.01**, in particular, shows the creep response of an Al-5%Mg alloy reinforced by 26% in volume Al_2O_3 fibres [23], while
Figure 1253.12.02 (a) illustrates the steady-state dependence on applied stress for a 6061 alloy reinforced with 20% (in weight) SiC whiskers [24]. In both cases the high values of the stress exponent reflect the strengthening effect of reinforcements. **Figure 1253.12.02** (b) shows the creep response of a 2124 alloy reinforced with a 20% (in volume) of SiC whiskers [25], and of a 2024 alloy reinforced with 15% SiC particles. It is apparent from Figure 1253.12.02 (b) that when a sufficiently wide range of strain rates is considered, the typical "threshold like behaviour" is observed.

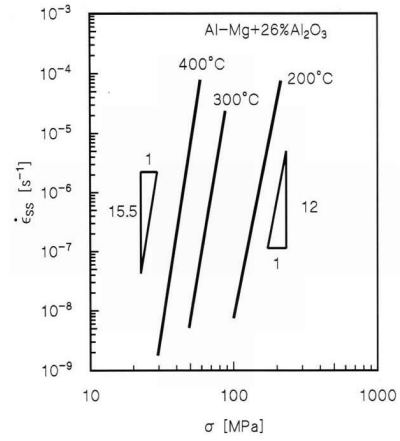

Steady state dependence on applied stress for an Al-Mg+Al_2O_3 fibres reinforced alloy at different temperatures [23].

TALAT Training in Aluminium Application Technologies | CREEP / 19 | 1253.12.01

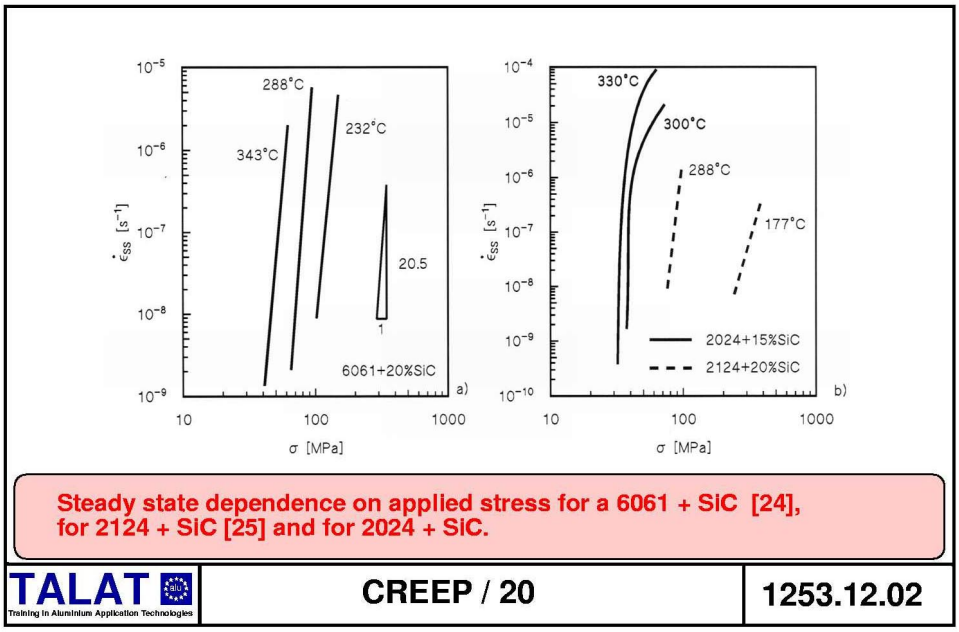

Steady state dependence on applied stress for a 6061 + SiC [24], for 2124 + SiC [25] and for 2024 + SiC.

1253.13 Final comments on the effectiveness and common features of creep- resistant aluminium alloys

The preceding discussion indicates that the only effective method to increase the low creep strength of Aluminium alloys is to introduce a stable distribution of particles or reinforcements. In this respect, the creep response of composites is reminiscent of particle-reinforced alloys obtained by powder metallurgy; both families of materials are characterised by very high values of the stress exponent and of the activation energy for creep, in particular when tested at the "intermediate" -stress regime. The increase in creep strength with respect to unreinforced materials is substantial, at least when temperature does not exceed 350°C, but a major concern is the relatively low fracture ductility, that in many cases does never exceeds 5%, while for the majority of the investigated conditions it is close to 1-2%.

Provided that a series of additional problems (ductility, toughness, fracture and fatigue, workability and, last but not least, cost) are solved, the current particle-reinforced alloys and composites could be the basis for the development of a new series of creep-resistant Aluminium light-weight materials. However, the current knowledge of the physical aspects of creep deformation is sufficiently detailed only for very simple alloys (pure Al, or Al-Mg solid-solution alloys), while major aspects of the creep response of particle-reinforced alloys or composites need to be more extensively studied and evaluated.

1253.14 Literature

1. Evans R.W. and B.Wilshire, Creep of Metals and Alloys, The Institute of Metals, London (1985) p.70.

2. Khatri S.C., A.Lawley and M.J.Koczak, Mater.Sci.Eng., A167 (1993) p.11.

3. Oikawa H. and T.G.Langdon, The Creep Characteristics of Pure Metals and Metallic Solid Solution Alloys, in "Creep behaviour of crystalline solids",

B.Wilshire and R.W.Evans eds., Pineridge Press, Swansea, U.K. (1985), p.33.

4. Yavari P. and T.G.Langdon, Acta metall., 30 (1982) p.2181.

5. Cadek J., Creep in Metallic Materials, Elsevier, Amsterdam (1988).

6. Wu M.Y. and O.D.Sherby, Acta metall., 32 (1984) p.1561.

7. Oikawa H., K.Sugawara and S.Karashima, Trans.Japan Inst.Metals, 19 (1978) p.611.

8. Oikawa H., K.Sugawara and S.Karashima, Scripta met., 10 (1976) p.885.

9. Yavari P., F.A.Mohamed and T.G.Langdon, Acta metall., 29 (1981) p.1495.

10. Li Y., S.R.Nutt and F.A.Mohamed, Acta mater., 45 (1997) p.2607.

11. Park K.T., E.J.Lavernia and F.A.Mohamed, Acta metall. mater., 42 (1994) p.667.

12. Griffith W.M., R.E.Sanders and G.J.Hildeman, Elevated Temperature Aluminium Alloys for Aerospace Applications, in "High Strength Powder Metallurgy Aluminium Alloys", M.J.Koczak and G.J.Hildeman eds., The Metallurgical Society of AIME, Warrendale, Pennsylvania (1982), p.209.

13. Millan P.P., High Temperature Powder Metal Aluminum Alloys to Small Gas Turbines, in "High Strength Powder Metallurgy Aluminium Alloys", M.J.Koczak and G.J.Hildeman eds., The Metallurgical Society of AIME, Warrendale, Pennsylvania (1982), p.225.

14. Pharr G.M., M.S.Zedalis, D.J.Skinner and P.S.Gilman, High Temperature Creep Deformation of a Rapidly Solidified Al-Fe-V-Si Alloy, in "Dispersion Strengthened Aluminum Alloys", Y.W.Kim and W.M.Griffith eds., TMS, Warrendale, Pennsylvania (1988) p.309.

15. Rosler J., R.Joos and E.Arzt, Met.Trans., 23A (1992) p.1521.

16. Kucharova K., A.Orlova, H.Oikawa and J.Cadek, Mat.Sci.Eng., A102 (1988) p.201.

17. Orlova A., K.Kucharova, J.Brezina, J.Krejci and J.Cadek, Scripta met.mater., 29 (1993) p.63.

18. Pandey A.B., R.S.Mishra, A.G.Parakdar and Y.R.Mahajan, Acta mater., 45 (1997) p.1297.

19. Hasegawa T., K.Minami and T.Miura, Creep behaviour of an Al-Al_2O_3 particle alloy produced by a mechanical alloying process, in "Creep and Fracture of Engineering Materials and Structures", R.W.Evans and B.Wilshire eds., The Institute of Metals, London (1990), p.159.

20. Cadek J., Acta Technica CSAV, 38 (1993), p.651.

21. Li Y. and F.A.Mohamed, Acta mater., 45 (1997) p.4775.

22. Li Y. and T,G.Langdon, Met.Trans., 28A (1997) p.1271.

23. Dragone T.L. and W.D.Nix, Acta metall.mater., 40 (1992) p.2781.

24. Nieh T.G., Met.Trans., 15A (1984) p.139.

25. Nardone V.C. and J.R.Strife, Met.Trans., 18A (1987) p.109.

1253.15 List of Figures

Figure No.	Figure Title (Overhead)
1253.02.01	Example of the typical shape of the creep curve
1253.03.01	Steady state creep rate vs. applied stress at constant T (a) or creep rate vs. T at constant stress (b); time to rupture vs. applied stress
1253.04.01	Time to rupture dependence on applied stress (a) and Larson-Miller master curve (b) for an experimental Al-Fe-V-Si-Er alloy
1253.05.01	Steady state dependence on applied stress for pure metals
1253.05.02	Mechanisms of climb controlled creep
1253.05.03	Mechanisms of purely diffusive creep
1253.05.04	Steady state dependence on applied stress for solid solution alloys
1253.06.01	Steady state dependence on applied stress for particle reinforced alloys and composites.
1253.07.01	Mechanisms of intergranular damage produced by grain boundary sliding
1253.08.01	Steady state dependence on applied stress for pure aluminium
1253.09.01	Steady state dependence on applied stress for Al-Mg solid solution alloys (T = 573 K)
1253.09.02	Steady state dependence on applied stress for Al-Mg solid solution alloys (T = 827K)
1253.10.01	Larson-Miller master curves for Aluminium and a 2xxx alloy
1253.10.02	Steady state creep rate vs. applied stress for Al-Mg solid solution alloy and for 2024 alloy produced by powder metallurgy
1253.11.01	Steady state creep rate vs. applied stress for an Al-Fe-V-Si-Er alloy
1253.11.02	Steady state creep rate vs. applied stress for an Al-Fe-V-Si alloy
1253.11.03	Steady state creep rate vs. applied stress for an Al-Al_4C_3 particle reinforced alloy at different temperatures
1253.11.04	Steady state creep rate vs. applied stress for an Al-Al_2O_3 particle reinforced alloy at different temperatures
1253.12.01	Steady state creep rate vs. applied stress for an Al-Mg + Al_2O_3 fibres reinforced alloy at different temperatures
1253.12.02	Steady state creep rate vs. applied stress for a 6061 + SiC, for a 2124 + SiC and for a 2024 + SiC